Published in final edited form as:
J Neurosci Methods. 2013 January 30; 212(2): 190–194. doi:10.1016/j.jneumeth.2012.09.022.

The small co-chaperone p23 overexpressing transgenic mouse

Junli Zhang[1,2,#], **Patricia Spilman**[1,#], **Sylvia Chen**[1], **Olivia Gorostiza**[1], **Alex Matalis**[1], **Kayvan Niazi**[1,3], **Dale E. Bredesen**[1,4], and **Rammohan V. Rao**[1,*]

[1]The Buck Institute for Research on Aging, Novato, California 94945

[4]University of California, San Francisco, San Francisco, California 94143

Abstract

Studies from multiple laboratories have identified the roles of several ER stress-induced cell death modulators and effectors. Earlier, we described the role of p23 a small co-chaperone protein in preventing ER stress-induced cell death. p23 is cleaved by caspases at D142 to yield p19 (a 19kD product) during ER stress-induced cell death. Mutation of the caspase cleavage site not only blocks formation of the 19kD product but also attenuates the cell death process triggered by various ER stressors. Thus, uncleavable p23 (p23D142N) emerges as a reasonable candidate to test for potential inhibition of neurodegenerative disease phenotype that features misfolded proteins and ER stress. In the present work we report the generation of transgenic mouse lines that overexpress wild-type p23 or uncleavable p23 under the control of a ROSA promoter. These mice should prove useful for studying the role of p23 and/or uncleavable p23 in cellular stress-induced cell death.

Keywords

endoplasmic reticulum; p23; HSP90; caspase; programmed cell death; Alzheimer's Disease

1. Introduction

Cell death pathways triggered by misfolded proteins and other activators of endoplasmic reticulum (ER) stress display both cytochrome c/Apaf-1 independent and cytochrome c/Apaf-1 dependent activation of programmed cell death (pcd) (Di Sano et al., 2006; Morishima et al., 2002; Rao et al., 2002; Rao et al., 2001; Zhang and Armstrong, 2006). Studies from multiple laboratories have described the roles of several ER stress-induced cell death modulators and effectors (Breckenridge et al., 2003; Bredesen et al., 2006; Rao et al., 2004; Xu et al., 2005) through the use of biochemical, pharmacological and genetic tools. We recently identified p23, a small chaperone protein that participates in ER stress-induced cell death as a key player in the coupling of ER stress to programmed cell death (Chinta et al., 2008; Poksay et al., 2012; Rao et al., 2006). p23 modulates HSP90 chaperone activity by

[*]Address correspondence to RVR rrao@buckinstitute.org, The Buck Institute for Research on Aging, 8001 Redwood Blvd, Novato, California 94945, Tel: 415-209-2000, Fax: 415-209-2230.
[2]Gladstone Institutes, University of California, San Francisco, San Francisco, California 94143
[3]Abraxis Bioscience, Los Angeles, CA 90025
[#]These authors contributed equally to this work.

Disclosure Statement: No financial conflicts exist

coupling the ATPase activity of HSP90 to polypeptide dissociation. However, we found that a subpopulation of p23 that is not bound to HSP90 plays a key role in ER stress-induced apoptosis (Chinta et al., 2008; Poksay et al., 2012; Rao et al., 2006). In vitro, p23 is able to bind specifically to misfolded proteins and the chaperone activity of p23 prevents aggregation and accumulation of misfolded proteins. Using several complementary approaches including immunodepletion and down-regulating the expression of p23 by RNA interference resulted in enhanced ER stress-induced apoptosis, suggesting a role for p23 as an anti-apoptotic protein (Chinta et al., 2008; Poksay et al., 2012; Rao et al., 2006). p23 is cleaved by caspases to yield a p19 fragment during ER stress-induced cell death and blockage of the caspase cleavage site of p23 is associated with decreased cell death triggered by various ER stressors (Chinta et al., 2008; Poksay et al., 2012; Rao et al., 2006). Thus, uncleavable p23 (p23D142N; p23unc) emerges as a reasonable candidate to test for potential inhibition of any cellular stress leading to pcd or neurodegenerative disease phenotype that features misfolded protein and/or ER stress. The potential ameliorative effect may occur because of the inability of p23D142N to be cleaved by caspases during ER stress.

Here we describe the production of transgenic (Tg) mice that overexpress p23wt (wild-type p23) or the p23unc. No gross physical or pathological symptoms have been observed in either of the Tg p23 mice colonies. The availability of genetically modified mice expressing p23wt or p23unc will facilitate studies on their function under normal and pathological conditions.

2. Materials and methods

2.1. Constructs and Genotyping

All molecular biology reactions utilized enzymes and reagents from New England BioLabs unless otherwise noted. N-terminal human *Flag-p23* was subcloned into a pcDNA3 expression vector (Invitrogen) by PCR-amplification of *p23* using a 5′-*p23* FLAG BamH1 and a 3′-*p23* Not1 primer pairs (Rao et al., 2006). The amplified N-terminal *FLAG-p23* cDNA (p23wt) was excised using BamH1 and Not 1 restriction enzymes and ligated into the pcDNA3 expression vector. Using the QuikChange Site-Directed Mutagenesis Kit (Stratagene), *FLAG-p23unc* (p23D142N) mutant was generated (Rao et al., 2006). The sequences of all constructs were confirmed by DNA sequencing.

The cDNAs encoding the *p23wt* and *p23unc* were digested with NotI, blunted by the 5′->3′ polymerase activity of Phusion polymerase, digested by BamHI, gel purified (Qiagen) and ligated into a pBroad (Invivogen) vector preparation previously digested with EcoRI, blunted, and digested with BglII in a directional cloning scheme. Resulting clones for both *pBroad-p23wt* and *pBroad-p23unc* were confirmed by DNA sequencing.

Transgenic mice were produced by standard techniques (Hogan B, Costantini F, Lacy E: Manipulating the Mouse Embryo: A Laboratory Manual. 1986) by the Institute's Transgenic Core. Purified linearized DNA (1–2ng/ul) was injected into the pronuclei of fertilized oocytes derived from C57BL/6 X C57BL/6 mice. 179 *p23wt* and 178 *p23unc* injected oocytes were transferred to oviducts of pseudopregnant female mice that resulted in 26 mice and 29 mice respectively. Tail DNA from resulting mice was isolated using a DNeasy Tissue Kit (Qiagen). Genotyping of *p23wt* and *p23unc* mice were by PCR and included the primers *p23*-5′ (5′CAGTTGTCTCGGAGGAAGTGAT3′) and *BGPA*-3′ (5′CAGATGCTCAAGGCCCTTCATA3′). The reaction products were electrophoresed on a 1.5% agarose gel with ethidium bromide. Five *p23wt* and three *p23unc* transgenic founder mice were crossbred with the C57BL/6 mice to obtain transgenic lines.

2.2. Antibodies and Western blotting

Expression of transgene was confirmed by Western blot analysis. Dissected and frozen mouse hemi-brains were homogenized in ice-cold phosphate-buffered saline lysis buffer containing 0.05% Nonidet P-40, 0.25% sodium deoxycholate, 50 mmol/L Tris–HCl (pH 8.5), 100 nmol/L NaCl, 1 mmol/L EDTA (pH 8.0), complete mini cocktail protease inhibitor (Roche), and 2 mg/mL b-glycerol phosphate (Galvan et al., 2006). Samples were then centrifuged at 16,000 × g for 10 min at 4ºC and the resulting supernatant assayed for total protein concentration. 50–100 μg of protein from total extracts was used for SDS- PAGE and Western blot analyses as described earlier (Rao et al., 2002; Rao et al., 2001; Rao et al., 2006; Rao et al., 2004). Proteins were detected using FLAG antibody (1:1000, Sigma) to differentiate the p23wt or p23unc from the endogenous mouse p23. Since the ROSA promoter directs the expression of the transgene ubiquitously in all tissues, expression of the transgene was also checked in other tissues including liver and heart. Equal protein loading was confirmed by reprobing blots with GAPDH (glyceraldehyde-3-phosphate dehydrogenase) monoclonal antibody (1:50,000, Research Diagnostics). Protein levels between different lines were quantitated by densitometry.

2.3. Immunohistochemistry

Hemi-brains from transgenic and non-transgenic littermate mice were removed and snap frozen on powdered dry ice. Coronal cryosections (14um) were cut, mounted on glass slides, air-dried, and post-fixed for 30 minutes in 4% paraformaldehyde. A relatively short fixation was necessary to preserve FLAG antigenicity. Sections were then washed in PBS followed by PBST (phosphate buffered saline, 0.05% Tween 20). Non-specific antibody binding was blocked with 5% normal goat serum (NGS) in PBST for 1 hour at room temperature. The primary antibody, rabbit anti-FLAG (F7425, Sigma) was used at 1:200 in PBST; sections were incubated overnight at 4°C. After 2 washes in PBST, sections were incubated with goat anti-rabbit Alexafluor 488 at 1:300 in PBST for 1 hour at room temperature. After washes in PBST and PBS, sections were mounted with Prolong Gold (Invitrogen) and glass coverslips, and viewed under a Nikon FM microscope. Images were taken using Act 1 software at 40X. Images were taken in the visual cortex, striatum, hippocampus, and thalamus. As lipofucsin that could be mistaken for FLAG labeling was readily visible using either the red-orange or green filters, only cells with little or no lipofucsin were imaged.

3. Results

3.1. Production of p23wt and p23unc transgenic mice

Initially we generated the *p23wt* mice using a CMV promoter. Despite analyzing several lines, we failed to detect the p23 transgene or the expression of p23 protein by Western blotting. Hence we used the mouse ROSA-26 promoter, a native ubiquitous promoter that directs the expression of the transgene ubiquitously throughout embryonic development and in adult tissues (Fig 1). The ROSA promoter has been successfully used by a number of laboratories to create transgenic mice (Belteki et al., 2005; Kisseberth et al., 1999; Lepore et al., 2005) and we are also using this promoter to generate other transgenic mouse models that are currently under investigation. The polymerase chain reaction (PCR) technique was utilized for identifying and confirming the transgene integration. As shown in Fig. 2A, we identified five *p23wt* founder mice and three *p23unc* founder mice by genomic PCR using the 5′ and 3′ primer pairs. The number of *p23wt* or *p23unc* transgene copies integrated in the genome was also estimated by the *LightCycler* quantitative polymerase chain reaction (qPCR). The ratios of the p23 target gene copy number were calculated relative to that of the GAPDH reference gene. We estimated that both *p23wt* and the *p23unc* mouse carried 2~4copies of the transgene per genome. The offspring of matings between heterozygous *p23* (p23+/−) mice showed genotypes in a ratio consistent with mendelian transmission

3.2. Phenotype

No discernable abnormality in the appearance or behavior was evident in the newborn, juvenile young or adult p23wt or p23unc mice. Body size and weight of the p23wt or p23unc mice were not strikingly different; there were neither any gross morphological abnormalities nor any noticeable differences in feeding or drinking behavior. Histological sections through the brain were normal. Both p23wt and p23unc weaned at ~3 weeks of age and gained weight to an equal extent. Male and female Tg mice were fertile by 4–6 weeks of age and no abnormal socialization were observed in either of the Tg mice

3.3. Expression of the transgene

Several lines of p23wt and p23unc were produced in order to derive mice with medium to high level p23 expression, which is needed both for the phenotype and for accurate comparisons. Densitometric analyses of levels of expression of the p23 transgene showed two lines each that had medium to high expression of p23wt (Fig. 2B) and 3 medium and 2 high expressors of p23unc (Fig. 2C).

Immunohistochemical analysis was also carried out to detect the expression of the transgene in different areas of the brain. Perinuclear/cytoplasmic FLAG labeling indicating p23 expression was detected only in the Tg mice in most brain regions with the highest expression in cortex and thalamus as shown in Figure 3. However, p23 level is not appreciably expressed in the striatum in both p23wt or p23unc mice. This may be either be due to differences in post-translational modification that may mask the antigenic site or increased turnover in the cells of the striatum due to metabolic differences.

Since the ROSA promoter is a ubiquitous promoter that directs the expression of the transgene throughout embryonic development and in all tissues, we also checked the expression of p23 in other tissues. As shown in Fig 4, expression of p23wt and p23unc was only observed in the liver and heart of the Tg mice.

4. Discussion and conclusions

p23 is a small chaperone protein that is closely associated with HSP90 but acts in an HSP90-independent fashion to inhibit endoplasmic reticulum (ER) stress-induced cell death. Earlier we showed that immunodepletion of p23 or inhibition of p23 expression by siRNA resulted in enhancement of ER stress-induced cell death (Poksay et al., 2012; Rao et al., 2006). p23 is cleaved by caspases to yield a 19kD product during ER stress-induced cell death triggered by various agents (Chinta et al., 2008; Poksay et al., 2012; Rao et al., 2006). ER stress-induced cleavage of p23 at the D142 site resulting in the 19kD product abolishes the ability of p23 to act as an antiapoptotic protein, thus rendering cells more susceptible to pcd. Moreover we believe that the 19kD cleaved product may display proapoptotic activity analogous to proteins such as APP, Bcl-2 or Bid (Cheng et al., 1997; Li et al., 1998; Lu et al., 2000).

Mutation of the caspase cleavage site D142N not only abolishes p23 cleavage, in addition p23unc seems to act as a dominant gene and inhibit the function of the endogenous wild-type p23 protein. This is based on the in vitro data that we previously published showing that expression of the p23unc in cells is associated with decreased cell death triggered by various ER stressors (Poksay et al., 2012; Rao et al., 2006). We believe that p23unc which has a single amino acid substitution may act as a dominant gene and inhibit the function of the wild-type p23 protein by suppressing its function (Mercola et al., 1990).

Data from several different laboratories suggest a link between Alzheimer's disease that features misfolded Aβ, the unfolded protein response (UPR), and ER stress all leading to

neuronal cell death (Bredesen et al., 2006; Ferreiro et al., 2006; LaFerla et al., 2007; Lindholm et al., 2006; Selkoe, 2003; Tseng et al., 2007). Mice overexpressing the human APP695 minigene carrying the Swedish (K670N, M671L) and Indiana (V717F) familial AD mutations downstream of the platelet-derived growth factor B-chain promoter have been previously described (PDAPP mice) (Mucke et al., 2000). The PDAPP Tg APP mice represent a well established model of Alzheimer's disease (AD) as they exhibit several of the classical AD-related deficits including hippocampal synaptophysin-immunoreactive presynaptic densities, plaque formation, reduced dentate gyral volumes, astrogliosis and other cognitive abnormalities (Bales et al., 2006; DeMattos et al., 2002; Donovan et al., 2006; Galvan et al., 2006; Nguyen et al., 2008).

Interestingly, while we did not observe the 19kD caspase cleaved product in the Tg APP mice, an increase in GRP78 levels was noticed when compared with non-transgenic littermates indicative of ER stress in these Tg APP mice (Poksay et al., 2012). Thus, despite the absence of the 19kD caspase cleaved product the ER stress machinery and downstream signaling pathways including the death amplification loop may be nonetheless activated. Moreover, proapoptotic fragments arising from caspase substrates are unstable, may represent a transient species with short half lives and are regulated through their selective degradation (Galvan et al., 2006; Piatkov et al., 2012; Semple et al., 2007). Thus, we hypothesize that simply preventing the caspase cleavage of p23 at Asp142 may be sufficient to block some or all of the AD phenotypic features in the PDAPP Tg APP mice. It is for this reason that the p23D142N mutant, which also has a caspase inhibitory effect (Rao et al., 2006) is hypothesized to ameliorate the AD phenotype displayed by these mice including effects on synapse loss, dentate gyral atrophy, EPSPs, and other behavioral abnormalities. We shall determine the effect of p23D142N on the Alzheimer's phenotype in vivo by crossing the p23wt and p23unc with the PDAPP Tg mouse and evaluate the effects of these two p23-expressing transgenic mice on the Alzheimer's phenotype. Thus, taking into account all these observations p23D142N emerges as a reasonable candidate to test for potential inhibition of the Alzheimer's disease phenotype.

Acknowledgments

We thank members of the Bredesen laboratory for helpful comments and discussions, Dr. David Toft (Mayo Medical School, Rochester, MN) for the human p23 cDNA and Rowena Abulencia for administrative assistance. The work in this laboratory is supported in part by grants from the National Institutes of Health NS33376 (D.E.B. & R.V.R), AG034427-02 (D.E.B), Douglas and Ellen Rosenberg Foundation (D.E.B) and Stephen D. Bechtel Foundation (R.V.R).

Abbreviations

ER	endoplasmic reticulum
pcd	programmed cell death
Tg	transgenic

References

Bales KR, Tzavara ET, Wu S, Wade MR, Bymaster FP, Paul SM, Nomikos GG. Cholinergic dysfunction in a mouse model of Alzheimer disease is reversed by an anti-A beta antibody. J Clin Invest. 2006; 116:825–32. [PubMed: 16498501]

Belteki G, Haigh J, Kabacs N, Haigh K, Sison K, Costantini F, Whitsett J, Quaggin SE, Nagy A. Conditional and inducible transgene expression in mice through the combinatorial use of Cre-mediated recombination and tetracycline induction. Nucleic Acids Res. 2005; 33:e51. [PubMed: 15784609]

Breckenridge DG, Germain M, Mathai JP, Nguyen M, Shore GC. Regulation of apoptosis by endoplasmic reticulum pathways. Oncogene. 2003; 22:8608–18. [PubMed: 14634622]

Bredesen DE, Rao RV, Mehlen P. Cell death in the nervous system. Nature. 2006; 443:796–802. [PubMed: 17051206]

Cheng EH, Kirsch DG, Clem RJ, Ravi R, Kastan MB, Bedi A, Ueno K, Hardwick JM. Conversion of Bcl-2 to a Bax-like death effector by caspases. Science. 1997; 278:1966–8. [PubMed: 9395403]

Chinta SJ, Rane A, Poksay KS, Bredesen DE, Andersen JK, Rao RV. Coupling Endoplasmic Reticulum Stress to the Cell Death Program in Dopaminergic Cells: Effect of Paraquat. Neuromolecular Med. 2008; 10:333–42. [PubMed: 18773310]

DeMattos RB, Bales KR, Parsadanian M, O'Dell MA, Foss EM, Paul SM, Holtzman DM. Plaque-associated disruption of CSF and plasma amyloid-beta (Abeta) equilibrium in a mouse model of Alzheimer's disease. J Neurochem. 2002; 81:229–36. [PubMed: 12064470]

Di Sano F, Ferraro E, Tufi R, Achsel T, Piacentini M, Cecconi F. Endoplasmic reticulum stress induces apoptosis by an apoptosome-dependent but caspase 12-independent mechanism. J Biol Chem. 2006; 281:2693–700. [PubMed: 16317003]

Donovan MH, Yazdani U, Norris RD, Games D, German DC, Eisch AJ. Decreased adult hippocampal neurogenesis in the PDAPP mouse model of Alzheimer's disease. J Comp Neurol. 2006; 495:70–83. [PubMed: 16432899]

Ferreiro E, Resende R, Costa R, Oliveira CR, Pereira CM. An endoplasmic-reticulum-specific apoptotic pathway is involved in prion and amyloid-beta peptides neurotoxicity. Neurobiol Dis. 2006; 23:669–78. [PubMed: 16844381]

Galvan V, Gorostiza OF, Banwait S, Ataie M, Logvinova AV, Sitaraman S, Carlson E, Sagi SA, Chevallier N, Jin K, Greenberg DA, Bredesen DE. Reversal of Alzheimer's-like pathology and behavior in human APP transgenic mice by mutation of Asp664. Proc Natl Acad Sci U S A. 2006; 103:7130–5. [PubMed: 16641106]

Kisseberth WC, Brettingen NT, Lohse JK, Sandgren EP. Ubiquitous expression of marker transgenes in mice and rats. Dev Biol. 1999; 214:128–38. [PubMed: 10491262]

LaFerla FM, Green KN, Oddo S. Intracellular amyloid-beta in Alzheimer's disease. Nat Rev Neurosci. 2007; 8:499–509. [PubMed: 17551515]

Lepore AC, Bakshi A, Swanger SA, Rao MS, Fischer I. Neural precursor cells can be delivered into the injured cervical spinal cord by intrathecal injection at the lumbar cord. Brain Res. 2005; 1045:206–16. [PubMed: 15910779]

Li H, Zhu H, Xu CJ, Yuan J. Cleavage of BID by caspase 8 mediates the mitochondrial damage in the Fas pathway of apoptosis. Cell. 1998; 94:491–501. [PubMed: 9727492]

Lindholm D, Wootz H, Korhonen L. ER stress and neurodegenerative diseases. Cell Death Differ. 2006; 13:385–92. [PubMed: 16397584]

Lu DC, Rabizadeh S, Chandra S, Shayya RF, Ellerby LM, Ye X, Salvesen GS, Koo EH, Bredesen DE. A second cytotoxic proteolytic peptide derived from amyloid beta- protein precursor [see comments]. Nat Med. 2000; 6:397–404. [PubMed: 10742146]

Mercola M, Deininger PL, Shamah SM, Porter J, Wang CY, Stiles CD. Dominant-negative mutants of a platelet-derived growth factor gene. Genes Dev. 1990; 4:2333–41. [PubMed: 2279701]

Morishima N, Nakanishi K, Takenouchi H, Shibata T, Yasuhiko Y. An endoplasmic reticulum stress-specific caspase cascade in apoptosis. Cytochrome c-independent activation of caspase-9 by caspase-12. J Biol Chem. 2002; 277:34287–94. [PubMed: 12097332]

Mucke L, Masliah E, Yu GQ, Mallory M, Rockenstein EM, Tatsuno G, Hu K, Kholodenko D, Johnson-Wood K, McConlogue L. High-level neuronal expression of abeta 1–42 in wild-type human amyloid protein precursor transgenic mice: synaptotoxicity without plaque formation. J Neurosci. 2000; 20:4050–8. [PubMed: 10818140]

Nguyen TV, Galvan V, Huang W, Banwait S, Tang H, Zhang J, Bredesen DE. Signal transduction in Alzheimer disease: p21-activated kinase signaling requires C-terminal cleavage of APP at Asp664. J Neurochem. 2008; 104:1065–80. [PubMed: 17986220]

Piatkov KI, Brower CS, Varshavsky A. The N-end rule pathway counteracts cell death by destroying proapoptotic protein fragments. Proc Natl Acad Sci U S A. 2012; 109:E1839–47. [PubMed: 22670058]

Poksay KS, Banwait S, Crippen D, Mao X, Bredesen DE, Rao RV. The small chaperone protein p23 and its cleaved product p19 in cellular stress. J Mol Neurosci. 2012; 46:303–14. [PubMed: 21691801]

Rao RV, Castro-Obregon S, Frankowski H, Schuler M, Stoka V, Del Rio G, Bredesen DE, Ellerby HM. Coupling Endoplasmic Reticulum Stress to the Cell Death Program. AN Apaf-1-INDEPENDENT INTRINSIC PATHWAY. J Biol Chem. 2002; 277:21836–42. [PubMed: 11919205]

Rao RV, Hermel E, Castro-Obregon S, del Rio G, Ellerby LM, Ellerby HM, Bredesen DE. Coupling endoplasmic reticulum stress to the cell death program. Mechanism of caspase activation. J Biol Chem. 2001; 276:33869–74. [PubMed: 11448953]

Rao RV, Niazi K, Mollahan P, Mao X, Crippen D, Poksay KS, Chen S, Bredesen DE. Coupling endoplasmic reticulum stress to the cell-death program: a novel HSP90-independent role for the small chaperone protein p23. Cell Death Differ. 2006; 13:415–25. [PubMed: 16195741]

Rao RV, Poksay KS, Castro-Obregon S, Schilling B, Row RH, Del Rio G, Gibson BW, Ellerby HM, Bredesen DE. Molecular components of a cell death pathway activated by endoplasmic reticulum stress. J Biol Chem. 2004; 279:177–87. [PubMed: 14561754]

Selkoe DJ. Folding proteins in fatal ways. Nature. 2003; 426:900–4. [PubMed: 14685251]

Semple JI, Smits VA, Fernaud JR, Mamely I, Freire R. Cleavage and degradation of Claspin during apoptosis by caspases and the proteasome. Cell Death Differ. 2007; 14:1433–42. [PubMed: 17431426]

Tseng BP, Green KN, Chan JL, Blurton-Jones M, Laferla FM. Abeta inhibits the proteasome and enhances amyloid and tau accumulation. Neurobiol Aging. 2007

Xu C, Bailly-Maitre B, Reed JC. Endoplasmic reticulum stress: cell life and death decisions. J Clin Invest. 2005; 115:2656–64. [PubMed: 16200199]

Zhang D, Armstrong JS. Bax and the mitochondrial permeability transition cooperate in the release of cytochrome c during endoplasmic reticulum-stress-induced apoptosis. Cell Death Differ. 2006; 14:703–15. [PubMed: 17170750]

HIGHLIGHTS

- We report the generation of transgenic mouse lines that overexpress p23 (p23wt) or p23unc (p23D142N) under the control of a ROSA promoter.
- No discernable abnormality in the appearance or behavior was evident in the p23wt or p23unc mice.
- Immunohistochemical analysis revealed protein staining in several areas of the brain.
- The mice will prove useful for studying the role of p23 and/or uncleavable p23 in cellular stress-induced cell death.

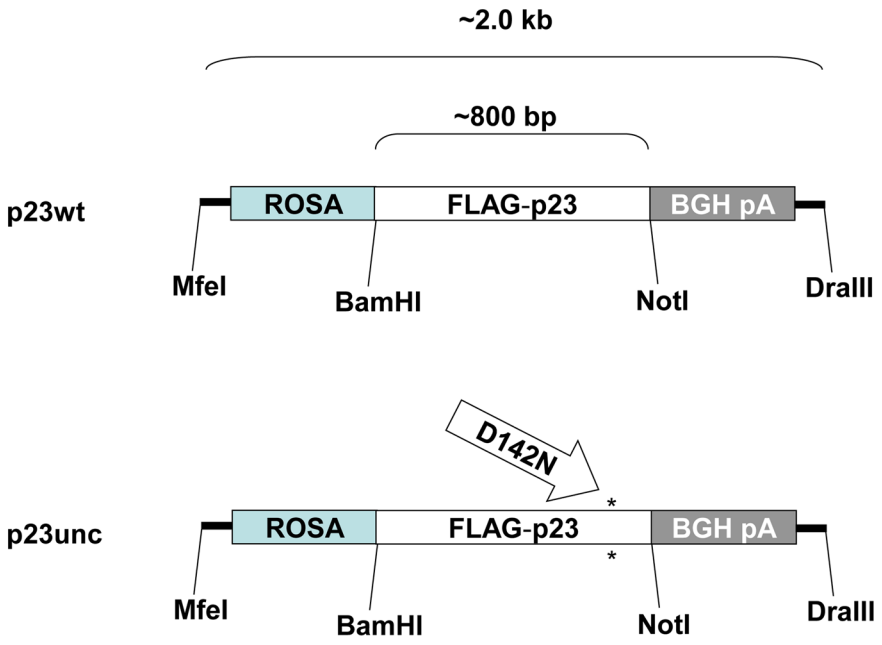

Fig. 1.

Schematic diagram of the constructs used for generating the transgenic mice. N-terminal Flag-*p23* (human) and Flag-*p23*D142N were each subcloned into a pcDNA3 expression vector (driven by the ROSA promoter) by PCR-amplification of each construct. Purified linearized DNA (1–2ng/ul) was injected into the pronuclei of fertilized oocytes derived from C57BL/6 X C57BL/6 mice. WTp23 (*p23wt)* and p23D142N (*p23unc*) transgenic mice were produced by standard techniques as mentioned in METHODS

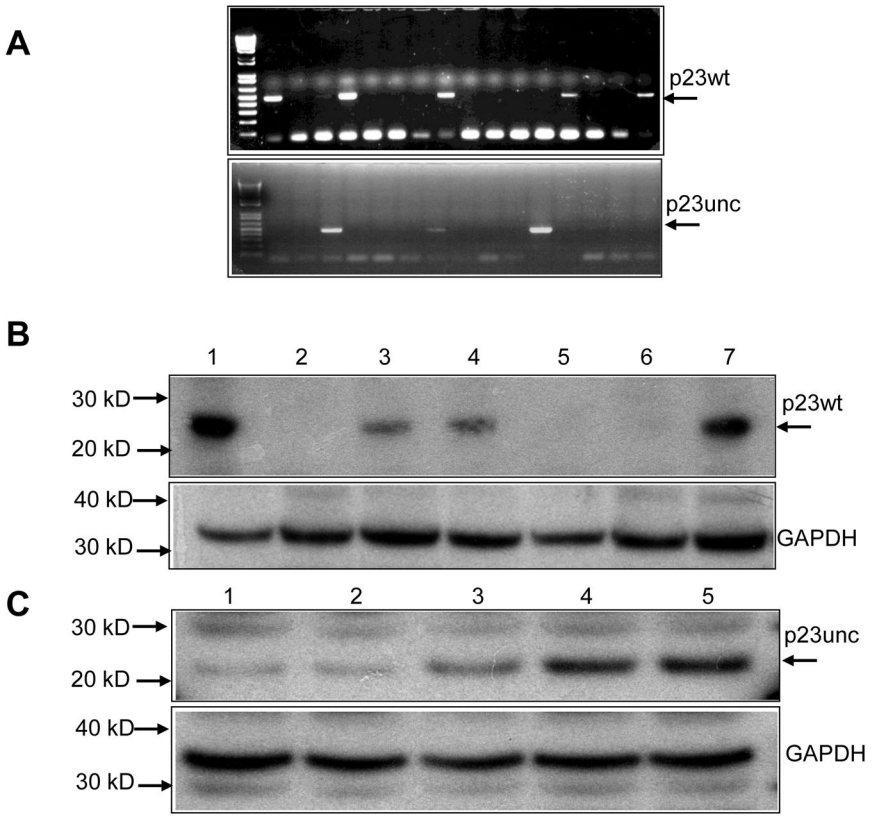

Fig. 2.

p23 transgene from tail DNA of mice. Tail DNA from mice was isolated and PCR was performed using the primers as mentioned in Methods. (A) Shown is a representative gel scan demonstrating the p23 transgene from tail DNA of mice. Five *p23wt* and three *p23unc* transgenic founder mice were chosen for establishing the transgenic lines. (B & C) Western blots showing the p23 expression in p23wt and p23unc mice. p23 protein was detected using anti-FLAG antibody. GAPDH served as a loading control.

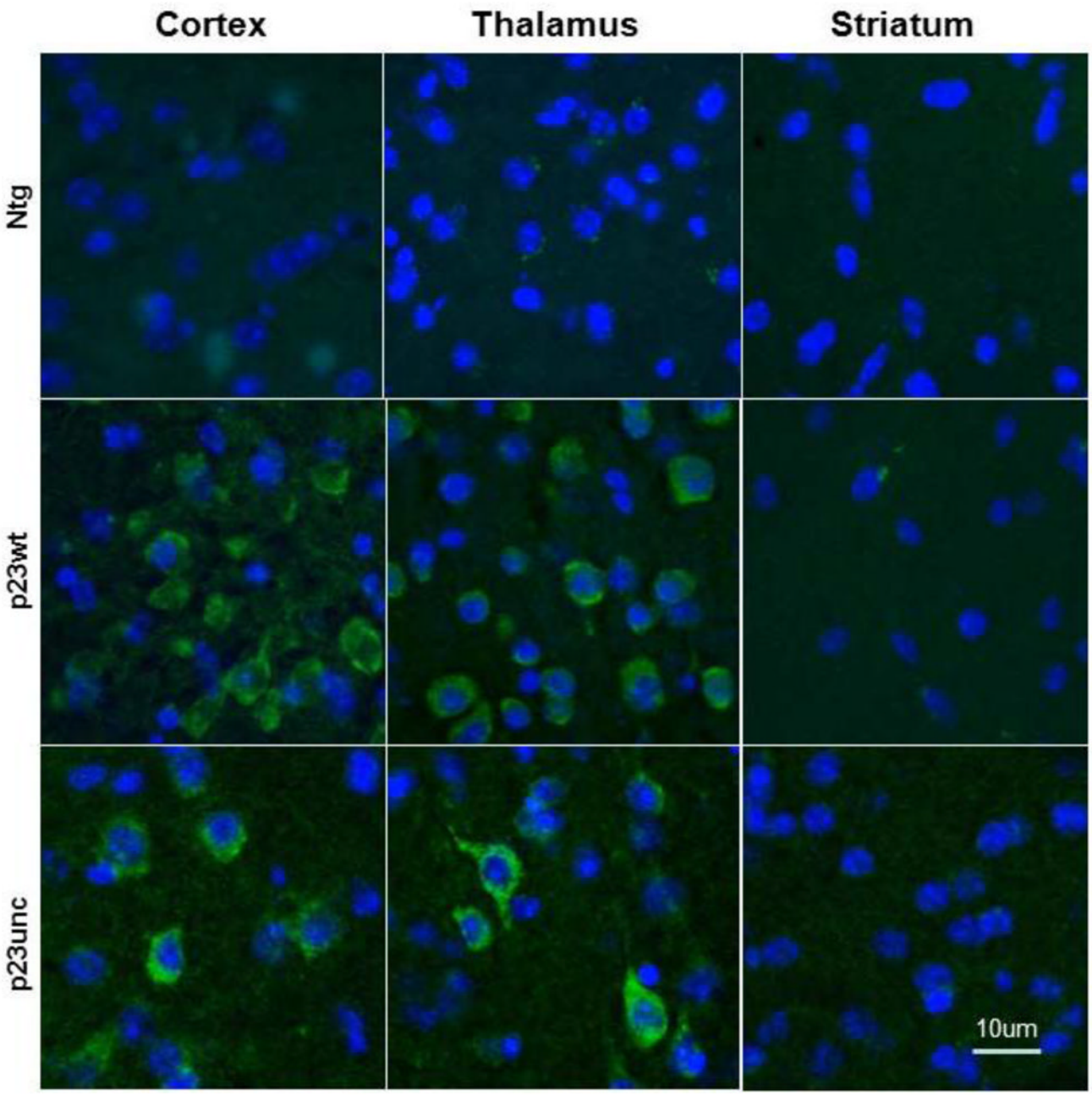

Fig. 3.

p23 staining by immunohistochemistry. Fluorescence immunohistochemistry on brain sections from p23wt or p23unc mice shows widespread p23 expression (green) in cortex and thalamus but not in the striatum. Staining is seen perinuclearly in most cells and in some cells bodies in all areas of the brain. Non transgenic (Ntg) mice showed low or no background staining. DAPI (blue) was used to stain nuclei.

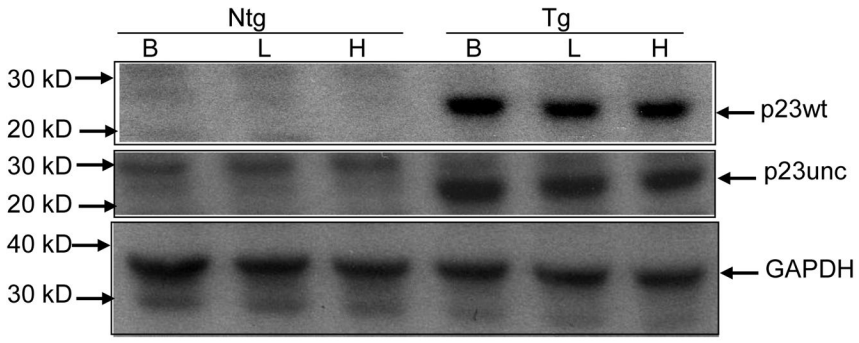

Fig. 4.

Expression of p23 in different tissues: Western blots showing expression of p23wt and p23unc protein in brain (B), liver (L) and heart (H) from transgenic (Tg) mice as compared to Non transgenic (Ntg) controls. p23 protein was detected using anti-FLAG antibody. GAPDH served as loading controls.